

Electronic spectroscopy in condensed media: The lowest $n-\pi^*$ transition of the solvated nitrite anion

Ajit Banerjee and Jack Simons^{a)}

Department of Chemistry, University of Utah, Salt Lake City, Utah 84112
(Received 7 November 1978; accepted 2 April 1979)

A general formalism developed in earlier publications for treating the electronic spectra of solvated anions is found to successfully describe the spectra of the nitrite anion in solvents of differing polarity (H_2O , EtOH, CH_3CN , DMF). The analysis presented supports the conclusions that the first excited state (1B_1) of the solvated nitrite anion is a bound state. The entire width of the spectra can be accounted for via a Frank-Condon progression alone. The predicted vibrational frequencies of the participating bending mode in the aqueous solution are found to be 1074 and 827 cm^{-1} in the ground ($X\,{}^1A_1$) and the excited (1B_1) states, respectively. These predicted frequencies have been further verified by *ab initio* calculations which simulate the gas-phase and solvated ion. The force constant for the ground state bending mode is found to be 9.8×10^{-11} dyne cm. in aqueous solution. The fitting procedure allows us to calculate an inhomogeneous broadening of 383 cm^{-1} for NO_2^- in water. These properties have been also calculated for the other solvents (EtOH, CH_3CN , and DMF) and trends in the changes of these quantities have been established.

I. INTRODUCTION

Recently, we developed a general theoretical framework for treating the electronic spectroscopy of solvated molecules and anions, in pure and mixed solvents.¹⁻⁴ In this series of articles, our goals are to test the predictive capabilities of our theoretical model and to gain valuable insights about the solute-solvent interactions by comparing the theoretically predicted and experimentally observed spectra.

The optical absorption and photodetachment spectra of the nitrite ion NO_2^- has been the subject of numerous studies.⁵⁻¹⁶ As early as 1940, Mulliken,⁵ and later Walsh,⁶ based on rather qualitative considerations, predicted that the low-lying electronic transitions of the nitrite ion would involve excitation from nonbonding lone pair or π orbitals to an antibonding π orbital. Experimental studies of crystal (NaNO_2) spectra by Sidman¹¹ and Tarwick and Eberhardt¹³ assign the weak lowest energy band near 26 000 cm^{-1} to an $n-\pi^*$ transition; the $\pi-\pi^*$ transition is assigned to the higher energy more intense band near 45 000 cm^{-1} . From the vibrational analysis of his experimental spectra, Sidman assigns vibrational frequencies of $\nu_1 = 1325 \pm 4$ cm^{-1} , $\nu_2 = 829 \pm 2$ cm^{-1} and $\nu'_1 = 1018 \pm 4$ cm^{-1} , $\nu'_2 = 632 \pm 4$ cm^{-1} , respectively, to the symmetric stretch and bending modes of the 1A_1 ground and 1B_1 excited states.

The most prominent feature of the absorption spectrum for the ${}^1A_1 \rightarrow {}^1B_1$ (i. e., $n-\pi^*$) transition is a progression corresponding to a frequency of 632 cm^{-1} (the bending vibration mode) in which the intensity maximum occurs in the fourth band ($v=0 \rightarrow \bar{v}=4$). The absorption and fluorescence spectra, measured by Sidman,¹¹ although similar, are not quite "mirror images"; this is consistent with the fact that the ratios of the frequency of the bending mode in the excited to that in the ground state is approximately 0.76. Strickler and Kasha¹⁴ studied at room temperature the optical absorption spectra of the nitrite anion in four different solvents of dif-

fering polarity and hydrogen bonding characteristics. The bands near 28 000 cm^{-1} were assigned by these authors to the $n-\pi^*$ transition whose maximum-absorption frequencies and intensities (ϵ) in the four different solvents are as follows: dimethylformamid (DMF), $\bar{\nu} = 26\,890$ cm^{-1} , $\epsilon = 27.6$; CH_3CN , $\bar{\nu} = 27\,000$ cm^{-1} , $\epsilon = 24.2$; EtOH, $\bar{\nu} = 28\,060$ cm^{-1} , $\epsilon = 29.5$; H_2O , $\bar{\nu} = 28\,200$ cm^{-1} , $\epsilon = 22.5$. This particular set of spectra will be the subject of the analysis of this paper.

Whereas the ground state of the nitrite anion is stable with respect to electron loss, in the gas phase, its excited states are autodetaching in character.^{15,16} It is generally known that, in condensed phases, the electronic states of anions become stabilized to an extent which often places the ground and low-lying excited states below the neutral molecule's ground state. As is discussed in more detail later in this paper, it is very probable that at least the first excited state (1B_1) of NO_2^- undergoes such stabilization in solution.

The gas-phase electron transmission (ETS) studies of Sanche and Schulz,¹⁶ as well as the laser photodetachment spectra of Herbst *et al.*,¹⁵ locates the ground state of NO_2^- about 2.4 eV below that of NO_2 . By analysis of the vibrational structure in the ETS spectra, Sanche *et al.* found the ground state (1A_1) symmetric stretch and bending vibrational frequencies to be 1032 and 524 cm^{-1} , respectively.¹⁷ These results may be compared with frequencies of 1325 and 829 cm^{-1} for the symmetric stretch and bending vibrations obtained in the crystal spectra of Sidman.¹¹ This decrease in the vibrational frequencies in going from the (NaNO_2) crystal to the gas phase should probably be ascribed to the "solvation" effects of the Na^+ ions which surround the nitrite ions. In our theoretical analysis, which is described in detail in a later section, we find that the solvation of NO_2^- by strongly interacting solvent molecules causes the NO_2^- vibrational frequencies to become even larger than in the crystal case. This observation is further supported by our analysis of the experimental aqueous phase NO_2^- spectrum and by quantum chemical calculations which we have performed, both of which are discussed later.

^{a)}Camille and Henry Dreyfus Fellow.

Given the fact that the 1A_1 state of NO_2^- lies 2.4 eV below the 2A_1 ground state of NO_2 , one can now employ information about the excitation energies of NO_2 to determine the stabilities of the excited anion states with respect to electron detachment. The absorption maxima in the ${}^1A_1 \rightarrow {}^1B_1$ ($n \rightarrow \pi^*$) transitions in the solution phase spectra of NO_2^- occur near 3.5 eV. Thus, unless there is a differential solvation of the anion over the neutral NO_2 plus a free electron amounting to more than 1.1 eV, the $n \rightarrow \pi^*$ transition will lie above the ionization threshold of NO_2^- in the solution phase. In other words, unless there is a solvent stabilization of NO_2^- which is 1.1 eV greater than that of the NO_2 plus a free electron [to form e^- (aqueous)], the detachment energy of NO_2^- (aqueous) will be less than $n \rightarrow \pi^*$ excitation energy. In this event, the $n \rightarrow \pi^*$ transition would be a bound-to-free transition. Delahay¹⁸ has reported blue shifts in anion photoionization spectra of 2–3 eV, so it is quite possible that at least the $n \rightarrow \pi^*$ transition involves a bound excited state. Our rather crude quantum chemical estimate, which is discussed in more detail in Sec. III, predicts the 1B_1 excited state to be stable relative to the neutral NO_2 plus a free electron by 4 eV.

Having presented this introduction concerning the nature of the electronic transitions and the problems we face in analyzing the solution phase spectra, we now undertake the task of carrying out the spectral analysis. In the following section, we give a brief review of the working equations of the theoretical model introduced in Refs. 1–3. Section III contains an analysis of relevant theoretical and experimental information on NO_2^- . Based on this analysis, physically reasonable models are introduced which serve to reduce the general equations of our theory to a computationally more tractable form which then is applied to the spectra of NO_2^- in four different solvents. In Sec. IV, we make our concluding remarks.

II. SPECTRAL LINE SHAPE THEORY

In earlier publications,^{1–4} we developed and implemented a rather general theory of optical absorption spectra of solvated molecules, anions, and charge-transfer complexes. In this section, we present a short sketch of the working equations of this theory, and we make a few comments to facilitate discussions of the approximations to be made for the specific systems at hand. For a more detailed discussion of the development of our working equations, the reader is referred to the articles cited above.

The electronic absorption intensity I as a function of frequency (ω) is related to the time correlation function $\langle F(t)F(0) \rangle$ of the electronic dipole operator F via a Fourier transform

$$I(\omega) = \frac{1}{2\pi} \int_{-\infty}^{\infty} dt \exp(i\omega t) \langle F(t)F(0) \rangle. \quad (1)$$

In principle, the time dynamics governing $F(t)$ involve the motion of both the solute (NO_2^- here) and the surrounding solvent molecules. As is shown in Ref. 1, the very complicated interactions between the solute and solvent molecules can be expressed, via the cumulant expansion technique,¹⁹ as a time-dependent effective

potential which acts on the “isolated” solute species, whose characteristics (geometry and vibrational frequencies) have been modified, allowing it to feel the static field provided by the solvent in equilibrium.¹ The effective potential contains the equilibrium averaged molecule–medium interaction as well as the terms arising from fluctuations in this interaction arising from fluctuations in the medium’s coordinates about their equilibrium values. Thus, the problem of studying dynamical properties of the solute in the solution is reduced to the study of a solute species which feels the presence of a time-dependent external field which no longer depends explicitly upon the coordinates of the medium.

In addition to introducing the concept of the effective external potential, our original development employed other physically motivated approximations to obtain an expression for $I(\omega)$ in terms of properties of the isolated solute and the solute–solvent effective potential. In implementing our theory, we assume that the former are known and we determine the latter by fitting the observed spectra to our equations. The approximations which must be introduced to arrive at a computationally useful theory are as follows: (i) The vibrational and rotational–translational degrees of freedom of the medium are assumed to be uncoupled, thereby allowing the thermal averaging, which appears in forming the cumulant approximation to the effective potential, to be performed separately over the respective coordinates and momenta. (ii) The electronic transition under study is assumed to occur in a time which is short relative to the time scale for variations in the solute’s or solvent’s vibrational, rotational, and translational coordinates. Thus, the intensities of each vibrational line in the electronic transitions explicitly in terms of Franck–Condon (FC) overlaps²⁰ between the vibrational functions of the absorbing species (labeled 0) and those of the species on which the excitation resides after the absorption takes place (labeled s).

For a localized transition ($s=0$), i. e., between the ground and the excited electronic state of the solute molecule, the FC factor corresponding to one of the participating vibrational modes λ_0 , having initial and final vibrational levels v_1 and \bar{v}_1 , is denoted as

$$F_{\lambda_0}(v_1, \bar{v}_1) = \langle v_1 \lambda_0 | \bar{v}_1 \lambda_0 \rangle. \quad (2)$$

The localized electronic–vibrational transition occurs at the energy $\Delta E_{e,v}$, which is expressed in terms of the electronic (E_0) and vibrational ($\epsilon_{v,\lambda}$) energies of the participating states as

$$\Delta E_{e,v} = \Delta E_e + \Delta E_v, \quad (3)$$

where

$$\Delta E_e = E^* - E_0 \quad (4)$$

and

$$\Delta E_v = \sum_{\lambda_0} (\epsilon_{v\lambda_0} - \epsilon_{v\lambda_0}). \quad (5)$$

Similar expressions for the FC overlaps and energy differences can be written for charge-transfer processes which involve excitation of an electron (at 0) to a neigh-

boring solute (or solvent) molecule at $s \neq 0$.

The general expression for $I(\omega)$ which results from making the above approximations (whose justification and treatment is given in detail in Refs. 1-3) gives the band shape function as a sum of the three following com-

ponents arranged according to their order of magnitude in the solute-solvent interaction strength:

$$I(\omega) = I^{(0)}(\omega) + I^{(1)}(\omega) + I^{(2)}(\omega), \quad (6)$$

where

$$I^{(0)}(\omega) = Z_v^{-1} \sum_{v_1, \bar{v}_1} \prod_{\lambda_0} \exp[-\beta \epsilon_{\lambda_0}(v_1)] [F_{\lambda_0}(v_1, \bar{v}_1)]^2 r_{00,0\lambda}^2 G(\omega, \Delta E_{e,v}, \sigma) \\ + Z_v^{-1} \int ds \rho(s, 0) \sum_{v_1, v_2} \prod_{\lambda_0, \lambda_s} \exp[-\beta \epsilon_{\lambda_0, \lambda_s}(v_1, v_2)] [F_{\lambda_0}(v_1, \bar{v}_1) F_{\lambda_s}(v_2, \bar{v}_2)]^2 r_{00, s\gamma}^2 G(\omega, \Delta E_{e,v}, \sigma), \quad (7)$$

$$I^{(1)}(\omega) = Z_v^{-1} \int dR \rho(R, 0) \sum_{\mu} \sum_{v_1, \bar{v}_1} \prod_{\lambda_0} \exp[-\beta \epsilon_{\lambda_0}(v_1)] (F_{\lambda_0})^2 r_{00,0\gamma} (r_{R\mu,0\gamma} \hat{h}_{00,R\mu} - r_{00,R\mu} \hat{h}_{R\mu,0\gamma}) \frac{(-1)}{\sigma^2} (\omega - \Delta E_{e,v}) G(\omega, \Delta E_{e,v}, \sigma) \\ + Z_v^{-1} \int dR dS \rho(R, 0) \rho(S, 0) \sum_{\mu} \sum_{v_1, v_2} \prod_{\lambda_0, \lambda_s} \exp[-\beta \epsilon_{\lambda_0, \lambda_s}(v_1, v_2)] (F_{\lambda_0} F_{\lambda_s})^2 \\ \times r_{00, s\gamma} (r_{R\mu, s\gamma} \hat{h}_{00,R\mu} - r_{00,R\mu} \hat{h}_{R\mu, s\gamma}) \frac{(-1)}{\sigma^2} (\omega - \Delta E_{e,v}) G(\omega, \Delta E_{e,v}, \sigma), \quad (8)$$

and

$$I^{(2)}(\omega) = Z_v^{-1} \int dR dR' \rho(R, 0) \rho(R', 0) \sum_{\mu\nu} \sum_{v_1, \bar{v}_1} \prod_{\lambda_0} \exp[-\beta \epsilon_{\lambda_0}(v_1)] (F_{\lambda_0})^2 r_{00,0\gamma} (r_{R\mu,0\gamma} \langle \delta h_{00,R'\nu} \delta h_{R'\nu,R\mu} \rangle + r_{00,R\mu} \langle \delta h_{R'\nu,0\gamma} \delta h_{R\mu,R'\nu} \rangle) \\ - 2r_{R\mu,R'\nu} \langle \delta h_{00,R\mu} \delta h_{R'\nu,0\gamma} \rangle \left[\frac{1}{\sigma^4} (\omega - \Delta E_{e,v})^2 - \frac{1}{\sigma^2} \right] G(\omega, \Delta E_{e,v}, \sigma) \\ + Z_v^{-1} \int dR dR' dS \rho(R, 0) \rho(R', 0) \rho(S, 0) \sum_{\mu\nu} \sum_{v_1, v_2} \prod_{\lambda_0, \lambda_s} \exp[-\beta \epsilon_{\lambda_0, \lambda_s}(v_1, v_2)] \\ \times (F_{\lambda_0} F_{\lambda_s})^2 r_{00, s\gamma} (r_{R\mu, s\gamma} \langle \delta h_{00,R'\nu} \delta h_{R'\nu,R\mu} \rangle + r_{00,R\mu} \langle \delta h_{R'\nu, s\gamma} \delta h_{R\mu,R'\nu} \rangle) \\ - 2r_{R\mu,R'\nu} \langle \delta h_{00,R\mu} \delta h_{R'\nu, s\gamma} \rangle \left[\frac{1}{\sigma^4} (\omega - \Delta E_{e,v})^2 - \frac{1}{\sigma^2} \right] G(\omega, \Delta E_{e,v}, \sigma). \quad (9)$$

Each of these three intensity factors contains localized ($r_{00,0\gamma}$) and charge transfer ($r_{00,s\gamma}$) electronic dipole matrix elements, involving ground (0) and excited (γ) states, particular FC factors, and associated Gaussian functions $G(\omega, \Delta E_{e,v}, \sigma)$ centered at $\Delta E_{e,v}$ whose σ accounts for the inhomogeneous broadening of each vibrational line. The higher-order terms [Eqs. (8) and (9)] also contain the solvent's pair distribution function $\rho(R, 0)$, the equilibrium averaged resonance integrals $\hat{h}_{R\mu, s\gamma}$ describing the intermolecular couplings (solute-solute and solute-solvent) which occur via the electronic Hamiltonian and involve the orbital μ of the solute species at R , and an orbital γ of the neighboring molecule at s . The second-order resonance couplings $\langle \delta h_{R\mu, s\gamma} \delta h_{R'\mu', s'\gamma'} \rangle$ measure correlations between fluctuations in $\hat{h}_{R\mu, s\gamma}$ and $\hat{h}_{R'\mu', s'\gamma'}$. The inhomogeneous broadening of each vibrational line arises in our theory via considerations of fluctuations in the (solvated) electronic energy levels of the solute caused by fluctuations in the solvent's instantaneous positions. Because the concentration of the nitrite ion is quite low in the experiments being analyzed here, and because the resonance coupling (h) has been shown to be negligibly small even in the most polar of the above solvents (H_2O), only the localized transitions appearing in Eqs. (6)-(9) need to be considered in treating the spectra of the nitrite ion in

the above four solvents. Under these circumstances, the expression to be used for $I(\omega)$ reduces to

$$I(\omega) = Z_v^{-1} \sum_{v_1, \bar{v}_1} \prod_{\lambda_0} \exp[-\beta \epsilon_{\lambda_0}(v_1)] \\ \times [F_{\lambda_0}(v_1, \bar{v}_1)]^2 r_{00,0\gamma}^2 G(\omega, \Delta E_{e,v}, \sigma). \quad (10)$$

Having completed this brief sketch of the pertinent ideas in our theory, we now turn to its application in analyzing the spectral band shape of the nitrite ion.

III. APPLICATION TO SOLVATED NITRITE ION SPECTRA

The utilization of the closed-form expressions for $I(\omega)$ given in Eq. (10) in an entirely predictive manner requires knowledge of the electronic-vibrational energy differences of the absorbing solute, the FC factors, the electric dipole transition integrals r , and the inhomogeneous broadening factor σ which is related to fluctuations in the solute's electronic energy levels $\sigma \sim \langle \delta h^2 \rangle$. All of this information is certainly not at hand within the currently available experimental data resources for the systems of interest here. Hence, our approach will be to employ as much experimental information as is available on those factors which relate to the isolated solute species and then to extract the remaining factors relating

to the solute-solvent interaction by fitting the experimental condensed-phase spectra to the functional form $I(\omega)$ given by our model. The past success of this approach in application to charge transfer³ and solvated anion spectra^{1,4} provides evidence that this method can yield valuable information about the nature of the anion-solvent interactions. We now put forth the experimental data which is presently available on NO_2^- and we present arguments which support some of the approximations mentioned in the preceding section for the specific system of interest here.

A. Justification of the neglect of charge transfer and solute-solvent resonance interaction

The nature of the ground and low-lying excited states of NO_2^- have been discussed by many authors. The nitrite ion in its ground state (X^1A_1) is described⁷⁻⁹ by the molecular orbital configuration $\Phi = (1b_2^2 1a_1^2 2a_1^2 3a_1^2 2b_2^2) \times 4a_1^2 5a_1^2 3b_2^2 1b_1^2 4b_2^2 1a_2^2 6a_1^2$. The orbital energies, within our (5s, 3p/4s, 3p) contracted Gaussian basis SCF calculation, are found for the valence-shell ($4a_1$ and higher) orbitals to be -0.61, -0.45, -0.42, -0.41, -0.22, -0.19, and -0.16 a.u. The $^1A_1 \rightarrow ^1B_1$ (i.e., $n \rightarrow \pi^*$) transition corresponds to an orbital excitation involving $6a_1 \rightarrow nb_1$ promotions $n > 1$. Our configuration interaction (CI) calculations on the 1B_1 state show that the most dominant configurations correspond to the excitations $\Phi(6a_1 - 2b_1)$, $\Phi(6a_1 - 3b_1)$, and $\Phi(6a_1 - 4b_1)$ with amplitudes in the 1B_1 state of 0.176, 0.782, and 0.592, respectively. The highest filled orbital of a_1 symmetry $6a_1$ is primarily a nonbonding orbital with the charge density divided in the ratio of 40:60 between the nitrogen and the two oxygen atoms of NO_2^- . Since the b_1 orbitals are linear combinations of N(p_x) and O(p_x) atomic orbitals, the transition $6a_1 \rightarrow nb_1$ would be an x -polarized allowed transition. An important feature of the $6a_1$ orbital, which will be used later in connection with hydrogen bonding to solvent molecules, is its sp hybridization involving the oxygen atomic orbitals. [The coordinate system and atomic coordinates are given in Fig. 2(a).] For the isolated NO_2^- anions, the charge densities residing in the oxygen p - [$O_1(p_x) + O_2(p_x)$] and s -type O(s) orbitals are found to have a ratio of 40. Strickler and Kasha found that the $X^1A_1 \rightarrow ^1B_1$ band maxima, which involves promotion of an electron from the $6a_1$ orbital, to be shifted to the blue in hydrogen-bonding solvents (H_2O and EtOH) when compared to the spectra in relatively inert solvents (CH_3CN and DMF). They concluded that this blue shift is due to the presence of hydrogen bonds involving the $6a_1$ orbital which makes it more difficult to remove the electron from this nonbonding lone-pair orbital.

To assess more quantitatively the nature and extent of such hydrogen bonding between the O atoms of the nitrite ion and H atoms of the solvent (H_2O) molecules, we performed SCF calculations on the $\text{NO}_2^-:\text{H}_2\text{O}$ dimer (C_{2v} symmetry) both in its most preferred geometry [shown in Fig. 2(b)] and in a few other geometries. The results of this minimum-energy geometry SCF calculation for the dimer suggest that the highest occupied orbital of a_1 symmetry (the $\text{NO}_2^- 6a_1$) has virtually no contribution from atomic orbitals centered on the H

atoms of the water molecule. Moreover, the ratio of the oxygen atoms p - to s -type orbitals in the $6a_1$ orbital of NO_2^- is found to increase to about 50. However, in both NO_2^- and $\text{NO}_2^-:\text{H}_2\text{O}$, the hybridization is essentially entirely p type. This means that the highest occupied orbital ($6a_1$) has been only slightly distorted (stretched) toward the H atoms of the water molecule. Even with such a minor distortion of the NO_2^- electron distribution, the binding energy for the $\text{NO}_2^-:\text{H}_2\text{O}$ in the preferred geometry was found to be ~ 15 kcal/mole, which is probably an underestimate because it results from a non-correlated SCF calculation. Because of the quite small charge polarization of the $6a_1$ orbital, we conclude that the hydrogen bonding in $\text{NO}_2^-:\text{H}_2\text{O}$ is mainly "electrostatic," arising from the Coulomb attraction of electrons in the $6a_1$ orbital of the NO_2^- and the H nuclei of the water molecule. This fact allows us to conclude that the resonance integrals $h_{\mu\nu}$, coupling the $6a_1$ orbital of NO_2^- to the a_1 -type symmetry H(s) orbitals of the water molecule, are small and can be safely neglected in our theory. Furthermore, since the NO_2^- concentration is small, the likelihood of finding two NO_2^- species as near neighbors is negligible; hence, all resonance couplings h and their fluctuations can be assumed to be negligible. In other words, the charge-transfer components of our theoretical model given in Eqs. (6)–(9) need not be taken into account. Of course, we also assume that the neglect of such resonance couplings will be equally valid for the case of less polar solvents (CH_3CN and DMF) for which the anion solvent interaction is even weaker.

For the above stated reasons, we believe that the experimental spectra can be appropriately analyzed in terms of the localized part of $I^{(0)}(\omega)$ as given in Eq. (10). Such simpler cases, i.e., those lacking the more involved anion-solute or anion-solvent interactions, provide us with opportunities to test the predictive capabilities our theory in its most rudimentary form.

B. Treatment of the vibrational factors in $I(\omega)$

Having examined pertinent information concerning the effects of the anion-solvent interactions on the nature of the $X^1A_1 \rightarrow ^1B_1$ transition, we now turn to the problem of modeling the various vibrational factors which occur in $I^{(0)}(\omega)$. These models serve to further reduce $I^{(0)}(\omega)$ to a computationally tractable form. Our next simplification is as follows: (a) We assume that the $n \rightarrow \pi^*$ transition is essentially bound to bound, or at least that the 1B_1 excited anion state is sufficiently long lived ($> 10^{-14}$ sec) that the contributions to the band shape $I(\omega)$ from the decaying-state nature can be ignored. As a further check for the validity of this assumption, we did a crude estimate (assuming pairwise additive potentials and using our calculated SCF energies at several different geometries of $\text{NO}_2^-:\text{H}_2\text{O}$) of the binding energy of $\text{NO}_2^-:6\text{H}_2\text{O}$ relative to $\text{NO}_2^-:6\text{H}_2\text{O}$. We estimate this differential stabilization to be of the order of 4 eV, which, if the 1B_1 state is stabilized by an amount close to that of the 1A_1 state, should be adequate to guarantee that the $n \rightarrow \pi^*$ transition involves a bound 1B_1 excited state. (b) We assume that the temperature of interest (room temperature) is low enough so that only the ground vi-

brational states of NO_2^- are initially occupied. Using the bending vibrational frequency of 829 cm^{-1} , one estimates a Boltzmann population of only 2% for the first vibrationally excited state; thus, this assumption is quite reasonable. (c) We assume that only one vibrational mode of NO_2^- is excited during the $n \rightarrow \pi^*$ transition. The experimental evidence given in Sidman's crystal spectra indicate that it is only the bending mode that participates in the absorption spectra. Although additional bands corresponding to the symmetric stretch were also detected, their intensities were too low to have any effect on the absorption band shape. (d) The FC factors for the participating bending mode and the corresponding energy differences are assumed to be well approximated within a harmonic oscillator model. The vibrational analysis of the solid phase spectra performed by Sidman reveals that the anharmonic corrections are small.

For the above stated reasons, we expect the harmonic approximation to be valid for our solution phase spectra as well. The FC factor arising in the ${}^1A_1 \rightarrow {}^1B_1$ transition involve the equilibrium angles and frequencies of the bending modes of the ground and excited electronic states, which are 829 and 632 cm^{-1} , respectively, in NaNO_2 crystal. Analysis of the solid-phase NaNO_2

spectra reveals that the excited 1B_1 potential surface is probably displaced relative to the 1A_1 ground state by an amount $\Delta\theta \cong 9^\circ$.

Within the harmonic oscillator approximation, the ground- and excited-state potential energy functions are taken to be

$$V_1(q) = b + \frac{1}{2}K_1(q+a)^2, \quad (11a)$$

$$V_2(q) = \frac{1}{2}K_2(q-a)^2, \quad (11b)$$

where $2a$ and b are the horizontal and vertical displacements of the two potential surfaces, respectively, and K_1 and K_2 are the respective force constants. The corresponding wave functions are

$$\Psi_n^{(1)}(q) = \left(\frac{\beta_1}{\sqrt{\pi} 2^n n!} \right)^{1/2} H_n[\beta_1(q+a)] \exp(-\frac{1}{2}\beta_1^2(q+a)^2), \quad (12a)$$

$$\Psi_m^{(2)}(q) = \left(\frac{\beta_2}{\sqrt{\pi} 2^m m!} \right)^{1/2} H_m[\beta_2(q-a)] \exp(-\frac{1}{2}\beta_2^2(q-a)^2), \quad (12b)$$

where H_n is a Hermite polynomial, and $\beta_i = (m\omega_i/\hbar)^{1/2}$, where ω_i is the vibrational frequency. McHale²² has calculated a general formula for the desired overlap (FC) factors within the harmonic oscillator model:

$$\langle \Psi_n^{(1)}(q) | \Psi_m^{(2)}(q) \rangle = F_\lambda(m, n)$$

$$= N \sum_{k=0}^{(n/2)} \sum_{l=0}^{(m/2)} \sum_{p=0}^{n-2k} \sum_{q=0}^{m-2l} \frac{[-0.25(1+f)]^{k+l}}{f^i} \frac{(m+n-2k-2l-p-q-1)!!}{k!l!p!q!(n-2k-p)!(m-2l-q)!} \left(\frac{2Xf^2}{1+f} \right)^{(1/2)P} \left(-\frac{2X}{1+f} \right)^{(1/2)Q}. \quad (13a)$$

Here, N is a constant of normalization

$$N = \exp\left(\frac{-Xf}{1+f}\right) (2^{(n+m+1)} n! m!) \left(\frac{f^{m+1/2}}{(1+f)^{m+n+1}} \right)^{1/2}, \quad (13b)$$

and $f = \omega_2/\omega_1$, where

$$\begin{aligned} (n)!! &\equiv 0, & \text{if } n \text{ is even,} \\ &1, & \text{if } n = -1, \\ n(n-2) &- 1, & \text{otherwise.} \end{aligned} \quad (13c)$$

The displacement factor (X) appearing above is related to the displacement $\Delta q = 2a$ between the electronic potential energy surfaces and the frequencies or force constants as

$$X = \frac{m\omega_1}{2\hbar} \Delta q^2 = \frac{K_1}{2\hbar\omega_1} \Delta q^2. \quad (14)$$

For the present case involving a bending vibration, the parameter X can be written in terms of the change in angle $\Delta\alpha (= \Delta q/q)$ and the corresponding angular force constant $f_1 (= K_1 q^2)$ as

$$X = \frac{f_1}{2\hbar\omega_1} \Delta\alpha^2. \quad (15)$$

The vibrational energy differences within the harmonic oscillator approximations are, of course,

$$\Delta E_\nu = \omega_2 \bar{\nu}. \quad (16)$$

Although these assumptions may be applicable to the particular system under consideration and not to the most general case, we believe that, for the given experimental conditions under which the spectra were taken, and given the currently available information for the anion states involved, the use of the zeroth order localized model $I^{(0)}(\omega)$ together with the above mentioned approximation is entirely justified.

After making these approximations, the localized part of the zeroth order band shape function of Eq. (10) can be written as

$$I^{(0)}(\omega) = r_{00,0}^2 \sum_{\bar{\nu}} [F_\lambda(0, \bar{\nu})]^2 G(\omega, \Delta E_{e,\nu}, \sigma). \quad (17)$$

Here the FC overlap $F(0, \bar{\nu})$ is given by Eqs. (13) and λ refers to the participating bending vibrational mode.

C. Results and discussion

As we now proceed to use the electronic band shape formula of Eq. (17) to analyze the experimental spectra of NO_2^- in different solvents, we need to determine the values of the vibrational (bending) frequencies in the ground (1A_1) and excited (1B_1) electronic states (ω_1, ω_2), the force constant f_1 for the ground vibrational state, and the change in the equilibrium angle $\Delta\alpha$, which together determine the dimensionless displacement parameter X according to Eq. (15). Recall that

Sidman *et al.* obtained values of 829 and 632 cm^{-1} for ω_1 and ω_2 , respectively, for solid NaNO_2 , whereas Sanche and Schulz obtained $\omega_1 = 524 \text{ cm}^{-1}$ for gas-phase NO_2^- . The experimental spectra of NO_2^- in all four solvents have very similar shapes except for their band maxima, which is blue shifted in the more polar solvents (H_2O , EtOH). All four spectra show a complete lack of any vibrational structure, and have quarter widths of 2682, 2460, 2400, and 2280 cm^{-1} , respectively, for solvents H_2O , EtOH, CH_3CN , and DMF. [Here we have reported widths at 3/4 height instead of more commonly used half-widths because the onset of the $\pi \rightarrow \pi^*$ transition (${}^1A_1 \rightarrow {}^1A_2$) overlaps the high energy tail of the ${}^1A_1 \rightarrow {}^1B_1$ transition under study.] From the intensity ratios of the observed spectra, one immediately calculates the relative dipole transition integrals $r_{00,0v}$ to be 0.988, 0.923, 1.000, and 0.871 in solvents DMF, CH_3CN , EtOH, and H_2O , respectively (normalized relative to the highest intensity for the solvent EtOH).

If we proceed to predict the $n \rightarrow \pi^*$ band shape using the crystal (NaNO_2) data given by Sidman [$\omega_1 = 829 \text{ cm}^{-1}$, $\omega_2 = 632 \text{ cm}^{-1}$, $\Delta E_{e,v} = 25960 \text{ cm}^{-1}$, $f_1 = 3.7822 \times 10^{-11}$ dyne cm, and $\Delta\alpha = 0^\circ$, for which Eq. (15) gives $X = 2.848$], the resultant $I(\omega)$ fails miserably. The widths are found to be only about 40% of the respective experimental spectral widths, and the line shape is predicted to be somewhat too skewed in comparison with the experimental spectra. Any one or more of several possibilities might account for this deficiency: (i) contributions from charge transfer components of $I(\omega)$, i. e., resonance couplings among clusters of the type NO_2^- : NO_2^- and NO_2^- : solvent may be present; (ii) contributions from decaying excited state life-time broadening; in Ref. 1, we have shown that the above two possibilities tend to increase the width of the calculated spectral band shape; (iii) contributions to $I(\omega)$ from the overlapping electronic transitions (${}^1A_1 \rightarrow {}^1B_1$ and ${}^1A_1 \rightarrow {}^1A_2$); (iv) contribution from two (bending as well as symmetric stretch) vibrational modes; and (v) the possibility that the vibrational frequencies of the ground and excited states (ω_1 and ω_2) and the $v = 0 \rightarrow \bar{v} = 0$ energy difference ($\Delta E_{e,v}$) in the solution phase may be quite different from those found in the NaNO_2 crystal spectra. The first two possibilities can be discarded based upon the earlier discussion, which employed results from our *ab initio* NO_2^- : H_2O calculations together with the fact that the NO_2^- concentration is small. Based on the analysis of the experimental spectra presented by Strickler and Kasha and by Sidman, the third and fourth possibility may also be discarded. One is then left to examine the possibility that ω_1 and ω_2 and $\Delta E_{e,v}$ might be considerably different in the four solvents studied than in the solid NaNO_2 or the gas-phase NO_2^- .

It has been noted by Rodloff¹² and by Sidman¹¹ that the crystal spectra of NO_2^- can be significantly altered when the environment of the NO_2^- ion is changed. For example, in the crystal spectra of CsNO_2 (at 77 °K), the $n \rightarrow \pi^*$ band is broader than for NaNO_2 and the vibrational structure is no longer resolved. In dilute mixed crystals of NO_2^- in KBr and KCl at 77 °K, the $n \rightarrow \pi^*$ band is found to be broader than in NaNO_2 and the $v = 0 \rightarrow \bar{v} = 0$ transition was found to occur at 25100 cm^{-1} , which is

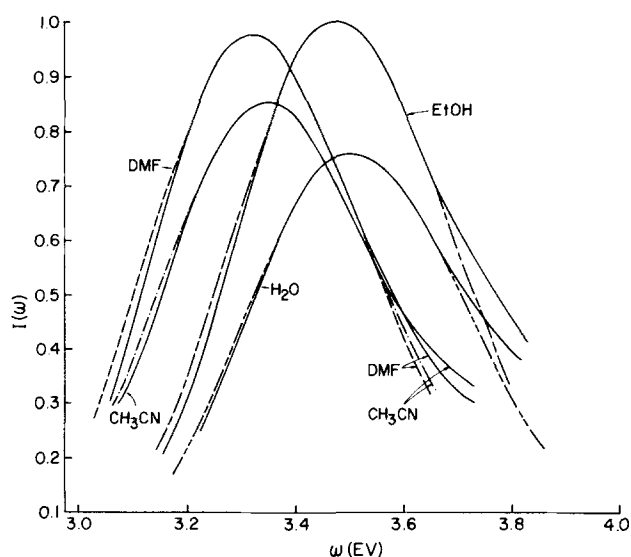


FIG. 1. Absorption band shape for nitrite anion in solvents H_2O , EtOH, CH_3CN , and DMF at room temperature: Solid—experimental, dashed—theoretical (shown only where different from experiment). Values of the parameter used for calculated spectra are, for solvent H_2O : $\omega_2 = 827 \text{ cm}^{-1}$, $f = 0.77$, $X = 5.70$, $\Delta E_{e,v} = 24893 \text{ cm}^{-1}$, $r = 0.871$, and $\sigma = 383 \text{ cm}^{-1}$; for solvent EtOH: $\omega_2 = 827 \text{ cm}^{-1}$, $f = 0.78$, $X = 5.50$, $\Delta E_{e,v} = 24752 \text{ cm}^{-1}$, $r = 1.00$, and $\sigma = 380 \text{ cm}^{-1}$; for solvent CH_3CN : $\omega_2 = 827 \text{ cm}^{-1}$, $f = 0.78$, $X = 5.45$, $\Delta E_{e,v} = 23692 \text{ cm}^{-1}$, $r = 0.923$, and $\sigma = 380 \text{ cm}^{-1}$; for solvent DMF: $\omega_2 = 827 \text{ cm}^{-1}$, $f = 0.79$, $X = 5.30$, $\Delta E_{e,v} = 23582 \text{ cm}^{-1}$, $r = 0.983$, and $\sigma = 380 \text{ cm}^{-1}$.

860 cm^{-1} lower in frequency than in NaNO_2 at 77 °K. Thus, we believe that it is quite reasonable for the solution-phase spectra to involve significant changes in the vibrational frequencies and $\Delta E_{e,v}$. In fitting the observed spectra to our Eq. (17), then, we shall permit ω_1 and ω_2 to assume values which are somewhat different from their solid-state (NaNO_2) values, but we must also be able to defend as reasonable the resultant optimal values found for ω_1 and ω_2 . The results of choosing $\Delta E_{e,v}$, ω_1 and ω_2 , X , and σ to give an optimal fit of the aqueous NO_2^- spectra (shown along with the experimentally observed spectra in Fig. 1) are $\omega_2 = 827 \text{ cm}^{-1}$, $f = \omega_2/\omega_1 = 0.77$ (or $\omega_1 = 1074 \text{ cm}^{-1}$), $X = 5.7$, $\Delta E_{e,v} = 24893 \text{ cm}^{-1}$, and $\sigma = 383 \text{ cm}^{-1}$.

If this specific choice of molecular parameters does indeed provide a valid description of the solvated nitrite ion, it can be seen that hydration has produced significant changes in the bending frequencies [1073.8 and 826.8 cm^{-1} compared to 829 and 632 cm^{-1} , respectively, in NaNO_2 crystal and an average bending frequency of 524 cm^{-1} in the gas phase (1A_1)] and the electronic energy difference (24893 cm^{-1} compared to 25951 cm^{-1} in the solid state). Although these large changes in bending frequencies may be somewhat surprising at first sight, there are data which tend to support their validity. The ratio ω_2/ω_1 for the calculated spectra in H_2O is found to be 0.77, which compares well to the ratio of 0.76 for the NaNO_2 crystal spectra. We also note that this similarity suggests that both the ground and the first excited states of NO_2^- become stabilized in H_2O by roughly the same magnitude as they do in

NaNO_2 . To offer more evidence supporting the "observed" increase in frequencies in the solution phase, we performed several SCF calculations to simulate the potential energy curves (bending vibration) of the nitrite ion in the presence of H_2O [$\text{NO}_2^-:\text{H}_2\text{O}$ in its most preferred geometry is showing in Fig. 2(a)] and in the gas phase (NO_2^- alone). Although the absolute values of the force constants and frequencies calculated from this simulation may not be meaningful, since they are derived from SCF calculations which neglect electron correlation effects, the ratios of the vibrational frequencies should be more significant.

From the potential energy curves shown in Fig. 2(b), it is clear that the $\text{NO}_2^-:\text{H}_2\text{O}$ force constant (and frequency) are larger than the NO_2^- (gas phase) values. Table I shows the calculated SCF energies of NO_2^- and $\text{NO}_2^-:\text{H}_2\text{O}$ as a function of the bond angle ONO of the nitrite ion. The ratio of the gas-phase to "liquid-phase" vibrational frequencies from these two calculated potential curves was found to be 0.67, which does not compare badly to the value of 0.49 obtained from the experimentally observed gas-phase frequency of 524 cm^{-1} and our "fitted" liquid-phase bending frequency of 1073 cm^{-1} , especially when one remembers that our liquid phase $\text{NO}_2^-:\text{H}_2\text{O}$ calculation involved interaction with only one H_2O molecule. We feel that this calculation provides more evidence that the solvation of NO_2^- does indeed cause a substantial change in the bending frequency of NO_2^- . The red shift of 1068 cm^{-1} in $\Delta E_{e,v}$ which occurs in going from solid NaNO_2 to $\text{NO}_2^-(\text{aq})$ is not surprising in view of the fact that a similar trend has been observed in crystals containing larger cations (C_3^+ or K^+) and the nitrite anion.

The resultant optimal value of $X(=5.7)$ contains infor-

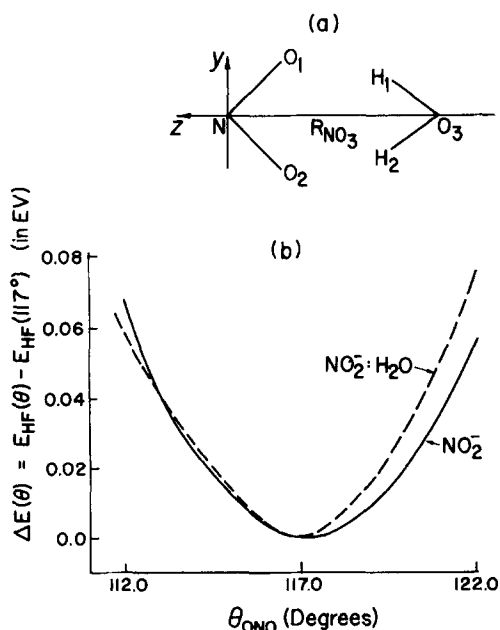


FIG. 2. (a) Minimum energy geometry for $\text{NO}_2^-:\text{H}_2\text{O}$ system, $R_{\text{NO}_3}=6.5$ bohr. (b) Potential energy curves as a function of the angle ONO of the nitrite ion for $\text{NO}_2^-:\text{H}_2\text{O}$ and NO_2^- systems. The differences $\Delta E = E_{\text{HF}}(\theta) - E_{\text{HF}}(117^\circ)$ is plotted to point out the differences in shapes of the curves.

TABLE I. Calculated potential energies for NO_2^- and $\text{NO}_2^-:\text{H}_2\text{O}$ as a function of the ONO angle of the nitrite ion.^a

ONO Angle (deg)	E_{HF} (hartree).	
	NO_2^-	$\text{NO}_2^-:\text{H}_2\text{O}$
112.0	-204.042007	-279.980615
115.0	-204.044061	-279.982238
116.6	-204.044488	-279.982687
117.0	-204.044510	-279.982709
118.0	-204.04438	-279.982484
119.0	-204.044189	-279.982116
122.0	-204.042419	-279.979966

^aThe calculated $\text{NO}_2^-:\text{H}_2\text{O}$ energies correspond to the axial geometry of Fig. 2(a).

mation about the bending frequency ω_1 of the ground state and the change in angle $\Delta\alpha$ between the equilibrium geometries of the solvated NO_2^- ion in the ground and excited states. As was suggested earlier, based upon the observation that the ratio ω_2/ω_1 remains unchanged and $\Delta E_{e,v}$ changes little in going from the liquid solvated NO_2^- to solid NaNO_2 , it is natural to assume that the stabilization and geometrical differences of the ground and excited states are approximately proportionate in the solution and solid phases. Hence, we infer that the (${}^1A_1 \rightarrow {}^1B_1$) angle change $\Delta\alpha(=9^\circ$ in NaNO_2) is probably nearly the same in the four liquids studied here as it is in solid NaNO_2 . Based on this premise, we calculate a force constant f_1 for the bending vibration in the ground electronic state of approximately 9.8×10^{-11} dyne cm (compared to 3.8×10^{-11} dyne cm for solid NaNO_2). The magnitude of the distortion factor ($X=5.7$) means that the excited (1B_1) potential energy surface for hydrated NO_2^- is displaced (in its angle) relative to the ground (1A_1) state to such an extent that the vertical transition from $v=0$ intersects the 1B_1 state at approximately the $\bar{v}=6$ level. This information about X together with the frequency ratio $\omega_2/\omega_1=0.77$ allows one to calculate that the observed band maximum in $\text{NO}_2^-(\text{aq})$ corresponds to the $v=0 \rightarrow \bar{v}=5$ transition.

In the absence of any of independent experimental information about the inhomogeneous broadening parameter σ , we adjusted σ to give the same lack of vibrational structure in our calculated spectrum as occurs in the observed liquid phase spectrum. The resultant value of $\sigma=383\text{ cm}^{-1}$ is similar to those found in our earlier treatment of the $\text{C}_6\text{H}_6\text{-I}_2$ charge transfer spectrum in liquid *n*-heptane at room temperature ($\sigma=400\text{ cm}^{-1}$) and the styrene anion in a glass at 77°K ($\sigma=410\text{ cm}^{-1}$), but much larger than the optimal value obtained for the cyclo-octatetraene anion in glass at 77°K ($\sigma=160\text{ cm}^{-1}$). Recall that the size of σ is dependent upon the degree of disorder in the solvent as well as the strength of the solvent-solute interaction.

Having explained in some detail the procedure for fitting the aqueous NO_2^- spectra to our Eq. (17), we are now prepared to consider the results of carrying out analogous treatments of the experimentally observed spectra involving the other three solvents EtOH, CH_3CN , and DMF. The spectral band maxima for the solvents H_2O

and EtOH appear at approximately the same frequencies (although with different intensities), which indicates that these solvents likely have similar interactions with the NO_2^- ion. Likewise, the fact that the band maxima and shapes for NO_2^- in DMF and CH_3CN are similar implies that these solvents have nearly the same interaction with NO_2^- . The fact that the band maxima for these two sets of solvents are separated by approximately 1200 cm^{-1} (H_2O and EtOH being to the blue) indicates that CH_3CN and DMF have weaker solvation forces.

The experimentally observed and calculated spectra of NO_2^- in H_2O , EtOH, CH_3CN , and DMF are shown in Fig. 1; the agreement between the calculated experimental spectra is quite good. The optimal values of the fitted parameters discussed above are given with Fig. 1. In analyzing this data for different solvents, there seems to be a trend towards decreasing X as one goes to the less strongly interacting solvents (DMF and CH_3CN). This means that the bending force constant of NO_2^- is somewhat smaller in these solvents. Another fact to be noted is the small change in the excited-to-ground state bending frequency ratios. This indicates that there is only a small change in the differential solvation of the two electronic states in the four solvents studied. The fact that the inhomogeneous broadening parameters σ are found to be nearly the same for all four solvents indicates that the amount of solvent disorder in the neighborhood does not vary significantly within this group of solutions.

IV. CONCLUSION

The results of the present analysis of the $n \rightarrow \pi^*$ absorption spectra of NO_2^- in four different solvents provide further evidence that the model developed in Refs. 1-3 can be useful for analyzing the electronic absorption spectra of molecular anions in condensed media. By comparing the experimentally observed NO_2^- spectra to our predictions [Eq. (17)], we have gained information about the bending vibrational frequencies of the ground and excited electronic states of the solvated ion, and about the geometry changes which accompany solvation. Through a comparison of the gas-, solid-, and liquid-phase values of the anion's properties, we have been able to establish trends in the frequencies, force constants, and effects of differential solvation. Using the fact that the FC profile of Eq. (17) is able to account for the entire width of the experimental spectra as well as *ab initio* quantum chemical estimates, we have been able to establish that the 1B_1 excited state is very probably a bound state. Due to the onset of the $\pi \rightarrow \pi^*$ (${}^1A_1 \rightarrow {}^1A_2$) transition which overlaps the high energy tail of the ${}^1A_1 \rightarrow {}^1B_1$ transition under study, there is an obvious

discrepancy between the calculated and the experimental spectra. It is possible to treat both transitions simultaneously using our more general Eq. (67) of Ref. 1, which calculates the intensity at a given ω from neighboring electronic transitions.

ACKNOWLEDGMENTS

Acknowledgment is made to the Donors of the Petroleum Research Fund, administered by the American Chemical Society, and to the National Science Foundation (Grant #CHE75-19576) for support of this research.

- ¹A. Banerjee and J. Simons, *J. Chem. Phys.* **68**, 415 (1978).
- ²J. Simons, *Int. J. Quantum Chem.* **13**, 553 (1978).
- ³J. McHale, A. Banerjee, and J. Simons, *J. Chem. Phys.* **69**, 1406 (1978).
- ⁴A. Banerjee and J. Simons, *J. Chem. Phys.* **69**, 5538 (1978).
- ⁵R. S. Mulliken, *Rev. Mod. Phys.* **14**, 204 (1942).
- ⁶A. D. Walsh, *J. Chem. Soc.* **1953**, 2266.
- ⁷K. L. McEwen, *J. Chem. Phys.* **34**, 547 (1961).
- ⁸E. Andersen and J. Simons, *J. Chem. Phys.* **66**, 2427 (1977).
- ⁹P. Benioff, *J. Chem. Phys.* **68**, 3405 (1977).
- ¹⁰G. Pfeiffer and L. C. Allen, *J. Chem. Phys.* **51**, 190 (1969).
- ¹¹J. W. Sidman, *J. Am. Chem. Soc.* **79**, 2669 (1957); **79**, 2675 (1957); *Chem. Rev.* **58**, 689 (1958).
- ¹²G. Rodloff, *Z. Phys.* **91**, 511 (1934).
- ¹³W. G. Trawick and W. H. Eberhardt, *J. Chem. Phys.* **22**, 1462 (1954).
- ¹⁴S. J. Strickler and M. Kasha, *J. Am. Chem. Soc.* **85**, 2899 (1963).
- ¹⁵E. Herbst, T. A. Patterson, and W. C. Lineberger, *J. Chem. Phys.* **61**, 1300 (1974).
- ¹⁶L. Sanche and G. J. Schulz, *J. Chem. Phys.* **58**, 479 (1973).
- ¹⁷We have chosen to report the average frequencies of each mole in the gas phase because, for solid phase spectra, Sidman¹¹ found that the anharmonic corrections were found to be negligible, and because we intend to use in our calculation a harmonic oscillator model to analyze the liquid phase spectra.
- ¹⁸L. Nemeč, L. Chia, and P. Delahay, *Can. J. Chem.* **55**, 1820 (1970).
- ¹⁹R. Kubo, *J. Phys. Soc. Jpn.* **17**, 1100 (1962).
- ²⁰G. Herzberg, *Electronic Spectra and Electronic Structure of Polyatomic Molecules* (Van Nostrand, Princeton, 1966).
- ²¹This estimate of differential stabilization of about 4 eV for $\text{NO}_2^-:6\text{H}_2\text{O}$ relative to $\text{NO}_2:6\text{H}_2\text{O}$ plus a free electron was arrived at using the difference in the detachment energies of $\text{NO}_2^-:\text{H}_2\text{O}$ and NO_2^- ($E_N = E_A + \text{detachment energy for the anion A}$). These differences in detachment energies for NO_2^- and three relatively preferred geometries above the xz symmetry plane [coordinate axis of Fig. 2(a)] for $\text{NO}_2^-:\text{H}_2\text{O}$ are 0.90, 0.88, and 0.85 eV. Thus, assuming that the excited state gets stabilized by a similar amount as the ground state of NO_2^- in the solution phase, we estimate the differential stabilization of the excited state of NO_2^- in solution relative to the ground state of NO_2 in gas phase to be about 4 eV.
- ²²J. McHale (private communication).